Minireview

Structural insights into the mechanism of proton pumping by bacteriorhodopsin

Teruhisa Hirai, Sriram Subramaniam*

Laboratory of Biochemistry, National Cancer Institute, Bethesda, MD 20817, USA

Received 19 February 2003; accepted 24 February 2003

First published online 1 May 2003

Edited by Bernard L. Trumpower

Abstract For over three decades, bacteriorhodopsin has served as a paradigm for the study of the mechanisms underlying ion pumping across biological membranes. It is perhaps among the simplest known ion pumps, which functions by converting light energy into an electrochemical gradient by pumping protons out of the cytoplasm. The combination of spectroscopic, biochemical and crystallographic studies on bacteriorhodopsin provides a unique opportunity to dissect the principal elements underlying the mechanism of transmembrane proton transport. Here, we provide a brief review of recent developments related to the determination of the structural changes during proton transport using crystallographic approaches. Taken together with previous spectroscopic and biochemical investigations, these studies allow the description of a detailed molecular mechanism of the main steps in vectorial proton transport by bacteriorhodopsin.

Key words: Proton pump; Conformational change; Retinal; Energy transduction

1. Introduction

Bacteriorhodopsin, a 27 kDa membrane protein, is a light-driven proton pump found in a specialized region of the inner membrane of the extreme halophile *Halobacterium salinarum*. In response to illumination, bacteriorhodopsin transports protons out of the cytoplasm and into the extracellular medium of this organism. The light sensor in bacteriorhodopsin is retinal, which is covalently bound to Lys216, a residue in the seventh transmembrane helix via a protonated Schiff base linkage. The effect of light on retinal is to change its configuration from the all-*trans* state to the 13-*cis* state, which triggers a remarkable series of protein conformational changes that ultimately result in the net translocation of a proton across the membrane. Retinal stays bound to the protein throughout this process, in contrast to the case of the visual rhodopsins in which the Schiff base linkage between retinal and the lysine residue is hydrolyzed soon after light absorption [1]. Bacteriorhodopsin is arguably the best-studied ion pump, and as a result of the extensive biochemical, biophysical and structural studies on the protein, an impressive amount of information has been gathered about the structure and function of this protein. Many comprehensive reviews that document different aspects of the function of this ion pump have been published [2–7]. Here, our goal is to highlight only the recent electron and X-ray crystallographic studies on bacteriorhodopsin, and to outline an integrated molecular mechanism that defines our present understanding of the main elements of vectorial proton transport.

2. The structure of bacteriorhodopsin

Bacteriorhodopsin has the distinction of having been the first membrane protein to have its structure determined at a resolution (~7 Å) that was high enough to recognize the arrangement of the helices in the membrane [8]. An atomic model based on the use of electron crystallographic approaches was first published in 1990 [9] and refined further in 1996 [10] to a resolution of ~3.5 Å. The discovery [11] that lipidic cubic phases could be used to crystallize bacteriorhodopsin was a major breakthrough that promised significant increases in resolution based on X-ray crystallographic studies of three-dimensional crystals. This expectation has indeed been fulfilled, as attested by the ensuing frenzied pace of publications reporting on the structure of bacteriorhodopsin at increasingly higher resolutions starting from 2.5 Å in 1997 [12] to 1.43 Å in 2002 [13]. There are 18 different sets of bacteriorhodopsin coordinates presently deposited in the Protein Data Bank, resulting from either electron microscopic or X-ray crystallographic studies of the unilluminated 'ground' state of wild-type bacteriorhodopsin (Table 1).

How similar are these structures? Fig. 1 shows a superposition of the Cα atoms of the 18 coordinate sets for bacteriorhodopsin. The plot of the superposed coordinates is reminiscent of the type of display that is usually presented in reports of structures derived by nuclear magnetic resonance (NMR) spectroscopy, and indeed there is some value in thinking about these structures in this light. There is excellent agreement among the different sets of coordinates on the path of the Cα backbone in the transmembrane regions (see also [14]) for an earlier comparison of structures derived using either electron microscopic or X-ray crystallographic methods). Almost all of the differences lie in the detailed conformations of side chains in the interior of the protein, and in the interpretation of the structure of the poorly ordered 'loop' regions connecting the transmembrane helices. Nevertheless, the more recent structural studies, beginning with the work of

*Corresponding author. Fax: (1)-301-480 3834.
E-mail address: ssl@nih.gov (S. Subramaniam).

0014-5793/03/$22.00
doi:10.1016/S0014-5793(03)00386-7

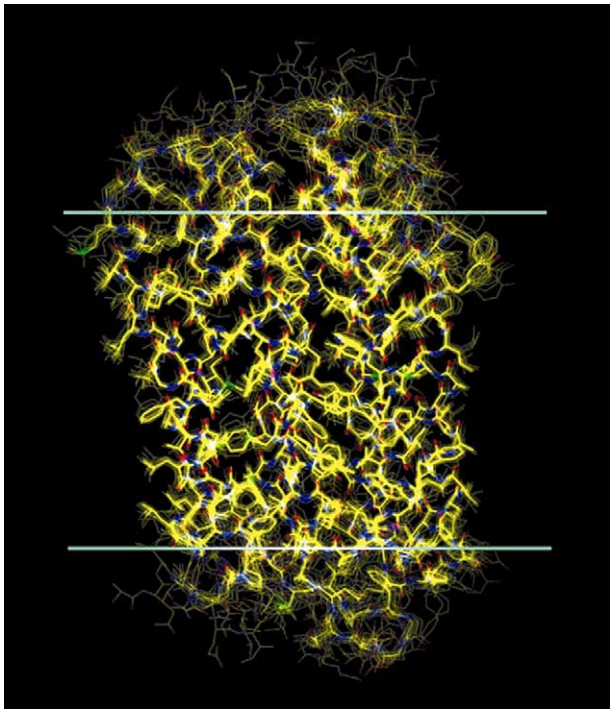

Fig. 1. Superposition of Cα atoms of 18 sets of bacteriorhodopsin coordinates obtained using either electron microscopic or X-ray crystallographic approaches. A least squares procedure was used to optimally align the Cα atoms of residues 9–29 (helix A), 43–60 (helix B), 81–94 (helix C), 108–128 (helix D), 134–152 (helix E), 178–191 (helix F) and 205–221 (helix G). These residues represent portions of the structure that are most ordered, and therefore most likely to be similar in the different coordinate sets. There is remarkable agreement among the different coordinate sets in the transmembrane region.

Luecke et al. [15], have provided remarkably detailed views of the organization of key residues and water molecules in the Schiff base region that will be essential for a quantitative understanding of the molecular mechanisms of light transduction.

A different perspective on the similarities among the different coordinates can be gleaned from the plot in Fig. 2, which presents the mean variation between structures (summarized in Table 1) as measured by the deviation of the positions of the Cα atoms of the transmembrane region of each structure as compared to an average structure derived from all of the coordinates. This deviation is plotted as a function of the resolution claimed for each of the reported structures. Inspection of the plot reveals the excellent agreement among all the structures posting resolutions better than 3 Å. It is to the credit of the early electron microscopic analyses that all of the X-ray structures have been determined by molecular replacement strategies using starting coordinates whose roots can be traced ultimately to the phases determined by electron crystallographic studies [9,10,16]. The plot also allows one to easily spot 1ap9 [12] as the one 'outlier' structure in the set. This is an instructive comparison, because of the errors inherent in the analysis of Pebay-Peroula et al. [12] resulting from the use of crystals with a high degree of twinning that were subsequently rectified in later studies, beginning with Luecke et al. [17].

3. The photocycle

Well before the description of an atomic model for bacteriorhodopsin, spectroscopic studies had shown that the key steps in light transduction could be described in terms of a photocycle that reported on changes in the local environment of retinal at different stages of proton transport [18]. Since this early work, the photocycle has been studied in great detail by a variety of optical and vibrational spectroscopic methods [19,20]. It is now generally accepted that the sequence of events involves formation of the intermediates K, L, M_1, M_2, N and O, with the same alphabetic notation used originally by Lozier et al. [18] to differentiate between the different spectroscopic states of retinal (Fig. 3). The only light-dependent event required for proton transport is retinal isomerization from the all-*trans* to the 13-*cis* configuration, which is complete on a picosecond time scale, corresponding to formation of the K intermediate in the photocycle. The remaining events in the photocycle occur thermally, on time scales ranging from microseconds (L and M_1 intermediates) to milliseconds (M_2, N and O intermediates). The transition from the M_1 and M_2 intermediates, which bisects the proton release and proton uptake halves of the photocycle, is thought to

Table 1
Models for the ground state of bacteriorhodopsin

PDB code	Method	Resolution (Å)	Residues in the model	Reference
1BRD	EM	3.5	8–32, 38–62, 74–100, 106–127, 137–157, 166–191, 202–225	[9]
2BRD	EM	3.5	7–227	[10]
1AT9	EM	3.0	2–231	[16]
2AT9	EM	3.0	6–227	[42]
1FBB	EM	3.2	4–227	[35]
1AP9	X-ray	2.35	7–225	[12]
1BRR	X-ray	2.9	3–232	[43]
1BRX	X-ray	2.3	6–152, 167–228	[17]
1C3W	X-ray	1.55	5–156, 162–231	[15]
1BM1	X-ray	3.5	7–227	[44]
1QHJ	X-ray	1.9	5–232	[45]
1E0P(A)	X-ray	2.1	5–232	[25]
1CWQ(A)	X-ray	2.25	2–239	[36]
1QM8	X-ray	2.5	2–230	Takeda et al., unpublished
1KGB	X-ray	1.81	5–156, 162–231	[46]
1IW6	X-ray	2.3	5–231	[24]
1KME	X-ray	2.0	5–231	[47]
1M0L	X-ray	1.47	5–156, 162–231	[13]

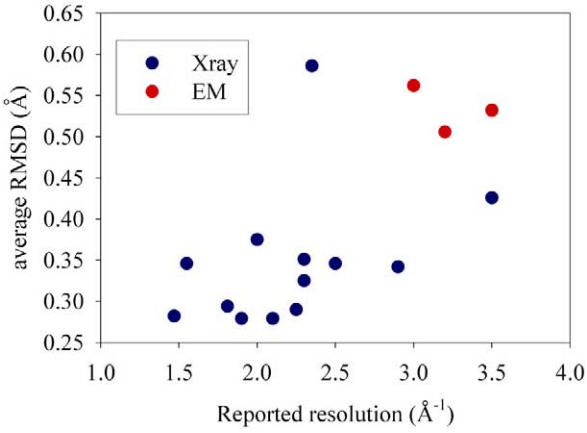

Fig. 2. Degree of self-similarity of the different coordinate sets. Sixteen sets were used; 1brd and 1at9 were excluded since they were replaced later by 2brd and 2at9, respectively. For each set of coordinates, the root mean square deviation with the 15 other sets was calculated using only the residues in the helical regions as noted in the legend to Fig. 1. The average of these 15 values is plotted as a function of the resolution associated with each coordinate set. The values are as follows: 0.532 Å (2brd), 0.426 Å (1bm1), 0.506 Å (1fbb), 0.562 Å (2at9), 0.342 Å (1brr(a)), 0.346 Å (1qm8), 0.586 Å (1ap9), 0.325 Å (1iw6), 0.351 Å (1brx), 0.290 Å (1cwq(a)), 0.279 Å (1e0p(a)), 0.375 Å (1kme), 0.279 Å (1qhj), 0.294 Å (1kgb), 0.346 Å (1c3w), 0.282 Å (1m0l).

represent the key event that ensures vectoriality of proton transport [21], i.e. to ensure that the proton is taken up from the cytoplasmic side and not from the extracellular side where the proton is released.

Determination of the structures of the intermediates generated by light absorption has been a primary goal of structural studies with bacteriorhodopsin in the last few years. This effort, carried out through the combined efforts of a number of laboratories using X-ray crystallography, electron crystallography and NMR methods, has been very successful. It has resulted in the generation of a comprehensive body of knowledge providing a detailed atomic picture of the rearrangements in retinal and the protein moieties during the photocycle. A list of atomic coordinates deposited in the PDB arising from experimental determinations of the structures of various intermediates are summarized in Table 2, along with references to the original publications. Below, we review the main findings from these studies.

3.1. K and L intermediates

Since the K intermediate appears ~1 ps after light absorption, almost all of the structural changes are localized to retinal and the region in its vicinity. Resonance Raman spectroscopic studies carried out over two decades ago [22] first established that the $C_{13}=C_{14}$ bond is almost fully rotated to the 13-*cis* configuration in the K intermediate, and the X-ray crystallographic studies are fully consistent with this conclusion. Minimal protein structural changes are observed, but the

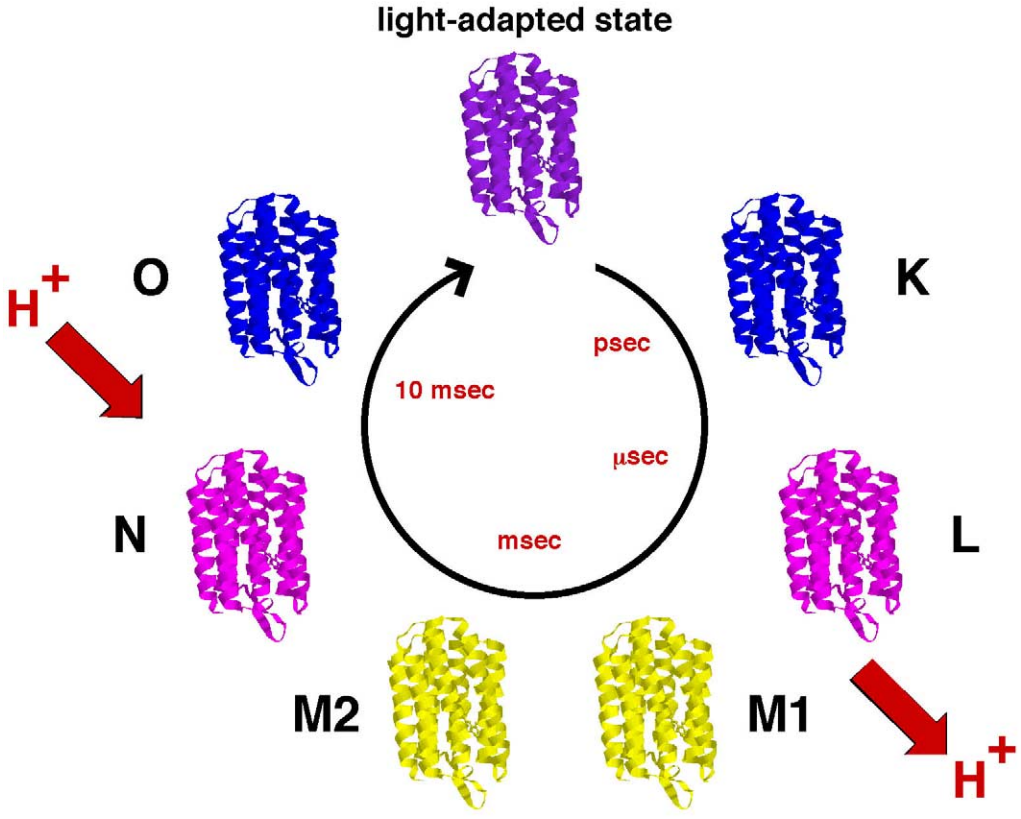

Fig. 3. The photocycle of bacteriorhodopsin. The intermediates generated upon illumination are shown, and the colors of the models shown roughly reflect the true colors of the intermediates. Proton release to the extracellular medium occurs with the decay of the L intermediate, and proton uptake from the cytoplasmic medium coincides with the decay of the N intermediate. The cycling time is ~10 ms at room temperature. Because the extent of the structural change at each intermediate is small on the scale of this drawing, all the cartoons shown are from the structure of wild-type bacteriorhodopsin.

minor rearrangements that occur appear to be localized to Asp85 and the hydrogen-bonded network connecting the Schiff base, water 402, Asp85 and Asp212 [13,23,24].

The L intermediate is formed on the microsecond time scale by thermal decay from the K intermediate. At this stage, the protein is poised to release the proton from the Schiff base to the key aspartic residue Asp85, which serves as the initial proton acceptor. There is no evidence for a large-scale protein conformational change that occurs with L formation, but the extent and nature of the small changes that might be expected to occur in the vicinity of retinal remain controversial [25,26]. However, it is very reasonable to expect that there would be some rearrangements near the extracellular region of the proton release channel, and the proposal of Royant et al. [25] of a role for a small bend in helix C is plausible and also consistent with the results from solid-state NMR studies [27]. The effect of the local rearrangements of the hydrogen-bonded network is to provide a pathway for proton release, and could involve reorientation of the guanidinium moiety of Arg82 so that it now points away from the interior and towards the exterior. Biochemical and spectroscopic analyses have shown that the formation of the L intermediate coincides with increased accessibility of the Schiff base to small hydrophilic reagents such as hydroxylamine that enter the protein from the extracellular side [28].

3.2. M_1, M_2 and M_N intermediates

The light-induced rearrangements of retinal and the protein region in its vicinity culminate in the release of a proton from the Schiff base to the extracellular medium. In the early literature on bacteriorhodopsin, most analyses presumed the existence of a single M intermediate. However, in the early 1990s, Janos Lanyi, Dieter Oesterhelt and their respective colleagues developed the idea that it was conceptually appropriate to think of the M intermediate in terms of two substates (M_1 and M_2) with similar absorption spectra but with significantly different protein conformations. Electron crystallographic studies of a variety of mutants trapped at different stages in the photocycle further supported this idea with the finding that the main protein conformational change in the photocycle coincides with the M_1 to M_2 transition [21]. This conclusion has been confirmed and extended by X-ray crystallographic studies of 3D crystals trapped in M_1-like states [26,29]. There are strong similarities in the nature of structural changes in the extracellular half of the protein in the L and M_1 states, but the most important difference lies in the altered protonation states of the key groups involved in proton transport: in the L state the Schiff base is protonated and Asp85 is deprotonated, while in the M_1 state, the Schiff base is deprotonated and Asp85 is protonated. This transferred proton stays on Asp85 until the very late stages of the photocycle, and the proton that is released into the extracellular medium comes from the H-bonded network between Asp85 and the extracellular surface. Residues Arg82, Glu194, Glu204 and water molecules in the vicinity make key contributions to this H-bonded network.

The combination of the altered configuration of retinal, the altered protonation states of the Schiff base and Asp85, and the changes in H-bonding in the extracellular half of the protein initiate the transition from the M_1 to M_2 states, and the main conformational change in the photocycle. Distinctions are sometimes made between the M_2 state in wild-type bacteriorhodopsin and the M_N state, which is the intermediate that accumulates in mutants where Asp96 is replaced by a neutral residue [30–32]. The similarities between these states far outweigh the fine differences, and the main point is that the state that accumulates after deprotonation of the Schiff base (M_2 or M_N) reflects the changed conformation of the protein.

What is the nature of the protein conformational change? Electron and X-ray crystallographic studies [33,34] of intermediates trapped after illumination suggested that changes at the cytoplasmic ends of helices F and G were likely to be the principal feature underlying the increased accessibility of the Schiff base to the cytoplasmic side. This proposal has been confirmed and extended in subsequent electron and X-ray crystallographic studies. An atomic model capturing the full extent of this conformational change has been obtained from electron crystallographic studies of 2D crystals of a mutant trapped in this state [35]. The key features of the structural change include the outward tilt of helix F with Pro186 serving as the hinge and an inward movement of the cytoplasmic end of helix G. These movements lead to an opening of the cytoplasmic part of the proton pathway allowing entry of a proton from the cytoplasm into the interior of the protein. All X-ray crystallographic studies of the M_2 or M_N intermediates using 3D crystals have also found evidence for conformational

Table 2
Models for the intermediate state of bacteriorhodopsin

PDB code (chain ID)	Method	Sample	State	Resolution (Å)	Residues in the model	Reference
1FBK	EM	D96G/F171C/F219L	M	3.2	4–228	[35]
1QKO	X-ray	WT	K	2.1	5–232	[23]
1QKP	X-ray	WT	K	2.1	5–232	[23]
1C8R	X-ray	D96N	Ground	1.8	5–156, 162–231	[15]
1C8S	X-ray	D96N	Late M (M_N)	2.0	5–153, 176–222	[15]
1F50	X-ray	E204Q	Ground	1.7	5–156, 162–231	[29]
1F4Z	X-ray	E204Q	Early M	1.8	5–156, 162–231	[29]
1E0P(B)	X-ray	WT	L	2.1	5–232	[25]
1CWQ(B)	X-ray	WT	M	2.25	2–239	[36]
1DZE	X-ray	WT	M	2.5	6–230	Takeda et al., unpublished
1JV7	X-ray	D85S	O	2.25	9–63, 78–232	[38]
1JV6	X-ray	D85S/F219L	O	2.0	9–63, 78–230	[38]
1KG8	X-ray	WT	Early M	2.0	5–155, 167–231	[46]
1KG9	X-ray	WT	Mock-trapped	1.81	5–156, 163–231	[46]
1IXF	X-ray	WT	K	2.6	5–231	[24]
1M0K	X-ray	WT	K	1.43	5–156, 162–231	[13]
1M0M	X-ray	WT	M_1	1.43	5–156, 162–231	[26]

changes in this region. Interestingly, in all X-ray crystallographic studies, the extent of this change is either muted significantly (e.g. [36]), or, as in the case of the work by Luecke et al. [32], the regions undergoing the conformational change are disordered. Nevertheless, the general consensus from every structural investigation of the conformational changes at the late M stages leaves little doubt that movements in helices F and G contribute to the rearrangements in the cytoplasmic part of the proton channel, and that this is an integral component of the mechanism of the proton uptake step in transport.

3.3. N and O intermediates

Following proton release, the Schiff base is reprotonated from the cytoplasmic side. The residue that provides the proton is Asp96, which maintains a high pK_a in the unilluminated state because of its relatively non-polar environment. The difference between the M_2 and N intermediates lies primarily in the reversal of the protonation state of the Schiff base and Asp96. Some site-specific mutants such as F219L display an accumulation of the N intermediate, and Vonck [37] took advantage of this to determine structural changes from an electron crystallographic analysis of 2D crystals of this mutant. The structural changes observed in illuminated crystals of this mutant are essentially identical to those reported by Subramaniam and Henderson [35] and completely consistent with the structural changes that Luecke et al. [32] might have seen in the M_N state of the D96N mutant had the 3D crystals used in their study not inhibited the occurrence of these changes. Further, two-dimensional projection maps of wild-type bacteriorhodopsin and several mutants trapped under conditions that favor M-like and N intermediates are also remarkably similar [21]. Taken together, these observations confirm that the proposal of Henderson et al. [9] that the protein conformations corresponding to the late M (i.e. M_2) and N intermediates must be similar was essentially correct.

Once the Schiff base is reprotonated, it remains for the internal proton donor Asp96 to be restored to its initial state by the uptake of a proton from the cytoplasmic side. Uptake of the proton generates the O intermediate, which in some respects has been more elusive to direct structural analysis than other intermediates. In wild-type bacteriorhodopsin, the O intermediate that accumulates is thought to contain retinal in a partially isomerized all-*trans* state. However, under physiologically relevant conditions the time scale of decay of the O intermediate is similar to its formation, resulting in very little accumulation of this intermediate. Because Asp85 is still protonated in the O intermediate, it is possible to consider the structures of mutants in which Asp85 is replaced by a neutral residue as analogs of the O intermediate, although the conclusions would clearly have to be interpreted with caution. Bob Glaeser and colleagues [38] have recently reported such experiments with the D85S and D85S/F219L mutants, and show that the main differences with the structure of unilluminated bacteriorhodopsin are almost exclusively in the extracellular half of the protein.

4. The molecular mechanism of proton transport

Knowledge of the protein structural changes in the photocycle and the many decades of biochemical and spectroscopic analyses provide a unique opportunity to piece together the mechanism of proton transport at an atomic level. In the dark, the protein exists as an equilibrium mixture of conformations in which the 13-*cis* 15-*syn* and all-*trans* 15-*anti* configurations of retinal are populated roughly equally. In the presence of continuous illumination, this equilibrium is shifted rapidly so that almost all of the molecules contain retinal in the all-*trans* configuration; this state is often referred to as the light-adapted state of bacteriorhodopsin. All of the experimental analyses on light-induced conformational changes are carried out starting with the light-adapted state. When the source of illumination is removed, the isomeric ratio is returned to the 13-*cis* and all-*trans* mixture in a slow process that takes many minutes [2].

In this light-adapted state, the protonated Schiff base sits in the vicinity of an extended H-bonded network, including the residues Asp85, Arg82, Asp212, Tyr57 and at least one structured water molecule (Wat402), although it is mainly stabilized by its interaction with Asp85, its primary counterion. The consequence of illumination is to isomerize retinal to the 13-*cis* 15-*anti* configuration, resulting in the formation of the K intermediate. The distinction between the 13-*cis* configuration generated in the photocycle and the 13-*cis* configuration present in the dark-adapted state lies in the *anti* vs. *syn* configuration of the C=N Schiff base linkage. This subtle difference has a profound effect on the environment of the Schiff base proton: in the 13-*cis* 15-*syn* configuration, the proton is pointed in almost the same direction as it is in the all-*trans* 15-*anti* configuration, and therefore, there is little change in the pK_a of the Schiff base. In contrast, in the 13-*cis* 15-*anti* configuration, the N–H proton is pointed in the opposite direction, towards a much less polar region of the protein. This isomerization thus leads to what is perhaps the single most important event in the photocycle: the reversal in the proton affinities [39] of the Schiff base and the proton acceptor Asp85, leading to the transfer of a proton from the Schiff base to Asp85. This event coincides with formation of the M_1 intermediate. The protonation of Asp85 triggers the release of a proton into the extracellular medium. No specific group seems to be the primary source of the released proton, which is thought to originate from the network formed by residues Arg82, Glu194, Glu204 and water molecules resident in the extracellular channel.

The essence of the functioning of bacteriorhodopsin as a vectorial proton pump is that the Schiff base is reprotonated from the cytoplasmic side and not the same side from which the proton is released. What is the mechanism that ensures the 'sidedness' of proton uptake? It has become clear that events at retinal play a critical role in this process. All of the theories proposed to account for vectoriality invoke changes in retinal structure that switch access of the Schiff base nitrogen from being connected to the extracellular H-bonded network in the first half of the cycle to the cytoplasmic H-bonded network in the second half of the cycle. Thus, based on NMR studies Herzfeld and colleagues have proposed that changes in the 'strain' of the retinylidene moiety are responsible for this switch (reviewed in [6,27]). Subramaniam and Henderson [35] proposed that measurable changes occurred in retinal curvature upon Schiff base deprotonation, and that the resulting displacement of the Schiff base nitrogen atom achieved the function of switching access from the extracellular to the cytoplasmic network. In a similar vein, Lanyi and colleagues (see for example [26]) have argued that torsional effects in

the geometry of retinal in the vicinity of the Schiff base are responsible for the switch in accessibility.

The upward displacement of retinal near the Schiff base brings the C-9 and C-13 methyl group into steric conflict with Trp182, a residue in helix F (Figs. 4 and 5). The presence of a proline residue (Pro186) one turn of the helix below Trp182 allows the translation of this steric pressure into the outward movement of the cytoplasmic helix F. The opening of the cytoplasmic channel via this outward motion of helix F and the associated rearrangements at the cytoplasmic end of helix G represent the dominant component of the protein conformational change that occurs during the photocycle, and set the stage for the final events in proton transport, beginning with the reprotonation of the Schiff base with the proton resident on Asp96. Once reprotonated, the Schiff base returns thermally to the all-*trans* state. In turn, this allows the 'resetting' of the conformational change and the reloading of

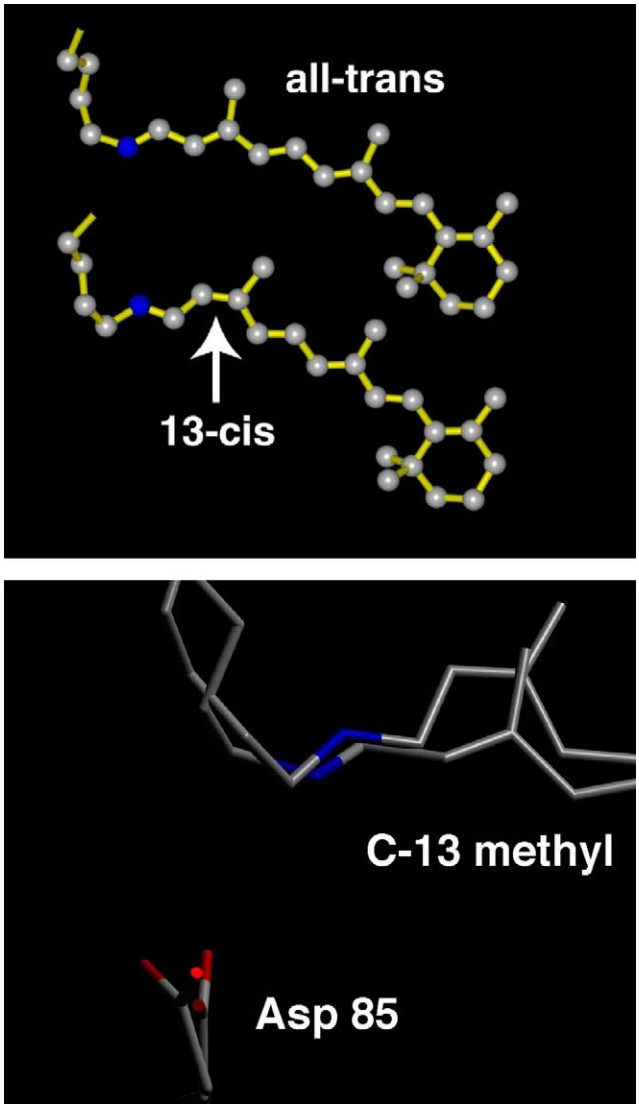

Fig. 4. Structures of all-*trans* 15-*anti*, and 13-*cis* 15-*anti* states of retinal illustrating the small change that occurs upon isomerization. Superposition of the structures of the unilluminated and illuminated states of the D96N mutant from the work of Luecke et al. [32] illustrating the upward movement of the C-13 methyl group in the 13-*cis* state.

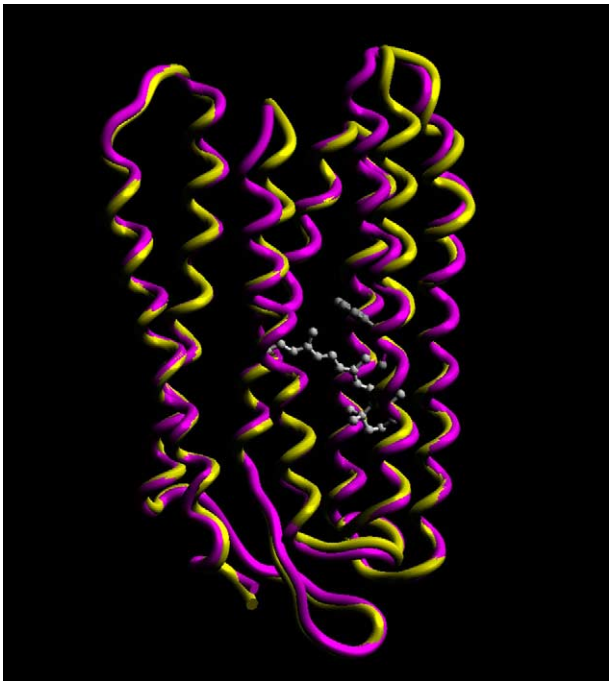

Fig. 5. Superposition of the structures for the closed and open states of bacteriorhodopsin. Residue Trp182, which is in close proximity to the C-9 and C-13 methyl groups of retinal, is shown. The upward movement of the Schiff base end of retinal results in steric pressure on Trp182 which, in combination with changes in electrostatic interactions due to deprotonation of the Schiff base, triggers events that set in motion the larger global protein conformational changes in the cytoplasmic channel.

Asp96 with a proton from the cytoplasmic side. Although thermal isomerization can occur in principle at any stage in the photocycle, its rate is greatly increased when both the Schiff base and Asp85 are protonated [40], and the local flexibility of the polyene chain is restricted by interactions with Leu93 and Val49 [41]. These conditions are met at this stage of the photocycle. With the return of the protein to the initial state, the pK_a of Asp85 is finally lowered, resulting in the transfer of the proton to the proton release complex. The molecule is now ready for the next cycle of light-driven proton transport.

5. Conclusion

The crystallographic snapshots of the various stages of the photocycle provide a fascinating glimpse of the inner workings of transmembrane proton transport. It is interesting to note that while the detailed description of the 'path' of the proton is valuable, it is also the case that all of the residues in the proton channel with the exception of Lys216 and Asp85 can be replaced without loss of the function of vectorial transport. In such mutants, alternative pathways must exist to get the proton to and from the Schiff base to the aqueous regions. Replacements of residues in the proton channel frequently do affect the kinetics, and sometimes even the sequence of proton release and uptake. However, it is abundantly clear that the subtle rearrangements of retinal and the global changes triggered by retinal movements are at the heart of proton pumping, and that the protein is remarkably tolerant to specific amino acid replacements at almost all locations.

References

[1] Khorana, H.G. (1992) J. Biol. Chem. 267, 1–4.
[2] Stoeckenius, W., Lozier, R.H. and Bogomolni, R.A. (1979) Biochim. Biophys. Acta 505, 215–278.
[3] Krebs, M.P. and Khorana, H.G. (1993) J. Bacteriol. 175, 1555–1560.
[4] Haupts, U., Tittor, J. and Oesterhelt, D. (1999) Annu. Rev. Biophys. Biomol. Struct. 28, 367–399.
[5] Lanyi, J.K. (2000) Biochim. Biophys. Acta 1459, 339–345.
[6] Herzfeld, J. and Lansing, J.C. (2002) Annu. Rev. Biophys. Biomol. Struct. 31, 73–95.
[7] Neutze, R., Pebay-Peyroula, E., Edman, K., Royant, A., Navarro, J. and Landau, E.M. (2002) Biochim. Biophys. Acta 1565, 144–167.
[8] Henderson, R. and Unwin, P.N. (1975) Nature 257, 28–32.
[9] Henderson, R., Baldwin, J.M., Ceska, T.A., Zemlin, F., Beckmann, E. and Downing, K.H. (1990) J. Mol. Biol. 213, 899–929.
[10] Grigorieff, N., Ceska, T.A., Downing, K.H., Baldwin, J.M. and Henderson, R. (1996) J. Mol. Biol. 259, 393–421.
[11] Landau, E.M. and Rosenbusch, J.P. (1996) Proc. Natl. Acad. Sci. USA 93, 14532–14535.
[12] Pebay-Peyroula, E., Rummel, G., Rosenbusch, J.P. and Landau, E.M. (1997) Science 277, 1676–1681.
[13] Schobert, B., Cupp-Vickery, J., Hornak, V., Smith, S. and Lanyi, J. (2002) J. Mol. Biol. 321, 715–726.
[14] Subramaniam, S. (1999) Curr. Opin. Struct. Biol. 9, 462–468.
[15] Luecke, H., Schobert, B., Richter, H.T., Cartailler, J.P. and Lanyi, J.K. (1999) J. Mol. Biol. 291, 899–911.
[16] Kimura, Y., Vassylyev, D.G., Miyazawa, A., Kidera, A., Matsushima, M., Mitsuoka, K., Murata, K., Hirai, T. and Fujiyoshi, Y. (1997) Nature 389, 206–211.
[17] Luecke, H., Richter, H.T. and Lanyi, J.K. (1998) Science 280, 1934–1937.
[18] Lozier, R.H., Bogomolni, R.A. and Stoeckenius, W. (1975) Biophys. J. 15, 955–962.
[19] Lanyi, J.K. (1993) Biochim. Biophys. Acta 1183, 241–261.
[20] Ebrey, T. G. (1993) in: Thermodynamics of Membrane Receptors and Channels (Jackson, M., Ed.), pp. 353–387, CRC Press, Boca Raton, FL.
[21] Subramaniam, S., Lindahl, M., Bullough, P., Faruqi, A.R., Tittor, J., Oesterhelt, D., Brown, L., Lanyi, J. and Henderson, R. (1999) J. Mol. Biol. 287, 145–161.
[22] Braiman, M. and Mathies, R. (1982) Proc. Natl. Acad. Sci. USA 79, 403–407.
[23] Edman, K., Nollert, P., Royant, A., Belrhali, H., Pebay-Peyroula, E., Hajdu, J., Neutze, R. and Landau, E.M. (1999) Nature 401, 822–826.
[24] Matsui, Y., Sakai, K., Murakami, M., Shiro, Y., Adachi, S., Okumura, H. and Kouyama, T. (2002) J. Mol. Biol. 324, 469–481.
[25] Royant, A., Edman, K., Ursby, T., Pebay-Peyroula, E., Landau, E.M. and Neutze, R. (2000) Nature 406, 645–648.
[26] Lanyi, J. and Schobert, B. (2002) J. Mol. Biol. 321, 727–737.
[27] Herzfeld, J. and Tounge, B. (2000) Biochim. Biophys. Acta 1460, 95–105.
[28] Subramaniam, S., Greenhalgh, D.A., Rath, P., Rothschild, K.J. and Khorana, H.G. (1991) Proc. Natl. Acad. Sci. USA 88, 6873–6877.
[29] Luecke, H., Schobert, B., Cartailler, J.P., Richter, H.T., Rosengarth, A., Needleman, R. and Lanyi, J.K. (2000) J. Mol. Biol. 300, 1237–1255.
[30] Kamikubo, H., Oka, T., Imamoto, Y., Tokunaga, F., Lanyi, J.K. and Kataoka, M. (1997) Biochemistry 36, 12282–12287.
[31] Oka, T., Yagi, N., Tokunaga, F. and Kataoka, M. (2002) Biophys. J. 82, 2610–2616.
[32] Luecke, H., Schobert, B., Richter, H.T., Cartailler, J.P. and Lanyi, J.K. (1999) Science 286, 255–261.
[33] Subramaniam, S., Gerstein, M., Oesterhelt, D. and Henderson, R. (1993) EMBO J. 12, 1–8.
[34] Koch, M.H., Dencher, N.A., Oesterhelt, D., Plohn, H.J., Rapp, G. and Buldt, G. (1991) EMBO J. 10, 521–526.
[35] Subramaniam, S. and Henderson, R. (2000) Nature 406, 653–657.
[36] Sass, H.J., Buldt, G., Gessenich, R., Hehn, D., Neff, D., Schlesinger, R., Berendzen, J. and Ormos, P. (2000) Nature 406, 649–653.
[37] Vonck, J. (2000) EMBO J. 19, 2152–2160.
[38] Rouhani, S., Cartailler, J.P., Facciotti, M.T., Walian, P., Needleman, R., Lanyi, J.K., Glaeser, R.M. and Luecke, H. (2001) J. Mol. Biol. 313, 615–628.
[39] Sampogna, R.V. and Honig, B. (1994) Biophys. J. 66, 1341–1352.
[40] Balashov, S.P., Imasheva, E.S., Govindjee, R. and Ebrey, T.G. (1996) Biophys. J. 70, 473–481.
[41] Delaney, J.K., Yahalom, G., Sheves, M. and Subramaniam, S. (1997) Proc. Natl. Acad. Sci. USA 94, 5028–5033.
[42] Mitsuoka, K., Hirai, T., Murata, K., Miyazawa, A., Kidera, A., Kimura, Y. and Fujiyoshi, Y. (1999) J. Mol. Biol. 286, 861–882.
[43] Essen, L., Siegert, R., Lehmann, W.D. and Oesterhelt, D. (1998) Proc. Natl. Acad. Sci. USA 95, 11673–11678.
[44] Sato, H., Takeda, K., Tani, K., Hino, T., Okada, T., Nakasako, M., Kamiya, N. and Kouyama, T. (1999) Acta. Crystallogr. D 55 (Pt 7), 1251–1256.
[45] Belrhali, H., Nollert, P., Royant, A., Menzel, C., Rosenbusch, J.P., Landau, E.M. and Pebay-Peyroula, E. (1999) Structure Fold. Des. 7, 909–917.
[46] Facciotti, M.T., Rouhani, S., Burkard, F.T., Betancourt, F.M., Downing, K.H., Rose, R.B., McDermott, G. and Glaeser, R.M. (2001) Biophys. J. 81, 3442–3455.
[47] Faham, S. and Bowie, J.U. (2002) J. Mol. Biol. 316, 1–6.